Available online at www.sciencedirect.com
SCIENCE DIRECT®
Journal of Magnetic Resonance 168 (2004) 53–65
JMR Journal of Magnetic Resonance
www.elsevier.com/locate/jmr

Subspace-based MRS data quantitation of multiplets using prior knowledge

T. Laudadio,[a,*] Y. Selén,[b] L. Vanhamme,[a] P. Stoica,[b] P. Van Hecke,[c] and S. Van Huffel[a]

[a] *Division ESAT-SCD (SISTA), Department of Electrical Engineering, Katholieke Universiteit Leuven, Kasteelpark Arenberg 10, Leuven-Heverlee 3001, Belgium*
[b] *Systems and Control Division, Department of Information Technology, Uppsala University, P.O. Box 337, Uppsala SE-751 05, Sweden*
[c] *Katholieke Universiteit Leuven, Biomedical NMR Unit, O & N Gasthuisberg, Herestraat 49, Leuven 3000, Belgium*

Received 13 October 2003; revised 22 January 2004

Abstract

Accurate quantitation of Magnetic Resonance Spectroscopy (MRS) signals is an essential step before converting the estimated signal parameters, such as frequencies, damping factors, and amplitudes, into biochemical quantities (concentration, pH). Several subspace-based parameter estimators have been developed for this task, which are efficient and accurate time-domain algorithms. However, they suffer from a serious drawback: they allow only a limited inclusion of prior knowledge which is important for accuracy and resolution. In this paper, a new method is presented: KNOB-SVD and its improved variant KNOB-TLS. KNOB-SVD is a recently proposed method, based on the Singular Value Decomposition (SVD), which allows the use of more prior knowledge about the signal parameters than previously published subspace-based methods. We compare its performance in terms of robustness and accuracy with the performance of three commonly used methods for signal parameter estimation: HTLS, a subspace-based method which does not allow any inclusion of prior knowledge, except for the model order; HTLSPK($\Delta f d_{eq}$), a subspace-based method obtained by incorporating in HTLS the prior information that the frequency differences between doublet components are known and the damping factors are equal; and AMARES, an interactive maximum likelihood method that allows the inclusion of a variety of prior knowledge. Extensive simulation and in vivo studies, using ^{31}P as well as proton MRS signals, show that the new method outperforms HTLS and HTLSPK($\Delta f d_{eq}$) in robustness, accuracy, and resolution, and that it provides parameter estimates comparable to the AMARES ones.

Keywords: Total least squares; Data subspaces; Magnetic resonance spectroscopy; Biochemical prior knowledge; Singular value decomposition

1. Introduction

The success of MRS as a non-invasive medical diagnostic tool depends on accurate estimation of the signal parameters. In particular, it is well known that the signal amplitudes are proportional to the concentration of the corresponding molecules in the observed volume and hence their accurate estimation provides a biochemical signature. Many time-domain algorithms for parameter estimation have been developed. On the one hand, interactive methods exist [1,2]. They are optimization-based methods which directly fit the MRS data to the model function by minimizing a certain criterion. They require a lot of user involvement but allow the inclusion of a variety of biochemical prior knowledge. Note that the relations among the resonance frequencies, amplitudes, and damping factors of multiplet components are usually known and by imposing such relations, the Cramer–Rao Bounds (CRBs) on the errors of estimated parameters are reduced [3,4].

On the other hand, so-called blackbox methods exist [5,6]. They directly estimate the model parameters by means of robust linear algebra tools such as the QR decomposition [7] (in which a given matrix A is decomposed as $A = QR$ where Q is an orthonormal matrix and R is an upper triangular matrix) and the SVD and can be fully automated, therefore requiring minimal user interaction. However, blackbox methods are

* Corresponding author. Fax: +32-16-321970.
E-mail address: Teresa.Laudadio@esat.kuleuven.ac.be (T. Laudadio).

1090-7807/$ - see front matter © 2004 Elsevier Inc. All rights reserved.
doi:10.1016/j.jmr.2004.01.015

characterized by a serious drawback in that they allow little inclusion of prior knowledge about the model parameters. A well-known blackbox method is HSVD [6]. It is a subspace-based parameter estimation method in which the noisy signal is arranged in a Hankel matrix **Y**. By truncating the SVD of the data matrix **Y** appropriately, a "signal" subspace and a "noise" subspace are computed and the pole information is extracted from the "signal" subspace basis. The performance of this method is improved by making use of the total least-squares (TLS) technique [8] instead of the least-squares (LS) technique, in solving the overdetermined set of equations derived from the signal subspace basis and the shift-invariant property. This variant is called HTLS [9] in the MRS literature and it possesses good resolution, parameter accuracy, and efficiency. However, HTLS does not use any prior knowledge about parameters in the data model, whose inclusion is important for further improvement of estimation accuracy and resolution. More accurate and efficient subspace-based methods have been developed by incorporating different types of prior knowledge (PK) in HTLS:

- HTLSPK(fd): frequencies and damping factors of some exponentials are known [10];
- HTLSPK(fp): frequencies and phases of some exponentials are known [11];
- HTLSPK(fdp): frequencies, dampings and phases of some exponentials are known [11];
- HTLSPK(p): phases of some exponentials are known [11];
- HTLSPK(Δfd_{eq}): the frequency differences between doublet components are known and the damping factors are equal [12,13].

In this paper, we present a new subspace-based method, called Knowledge Based Total Least Squares (KNOB-TLS), which is an improved variant of Knowledge Based Singular Value Decomposition (KNOB-SVD). KNOB-SVD was recently proposed in [14] and it allows the inclusion of significantly more prior knowledge in MRS data quantitation than the above mentioned methods. More precisely, we assume that the function used to model the measured data points of an MRS signal is the sum of K exponentially damped complex sinusoids

$$y_n = \sum_{k=1}^{K} a_k \mathrm{e}^{j\phi_k} \lambda_k^n + \epsilon_n, \quad n = 0, \ldots, N-1, \tag{1.1}$$

where the number of components K is assumed to be known, $\lambda_k = \mathrm{e}^{(-d_k + j2\pi f_k)\Delta t}$ represent the signal poles, (a_k, ϕ_k, d_k, f_k) are the amplitude, phase, damping and frequency of the kth component, Δt is the data sampling period, and ϵ_n is the noise term.

Our goal is to estimate the parameters (a_k, ϕ_k, d_k, f_k) from N given data samples $\{y_n\}_{n=0}^{N-1}$. As prior knowledge, we assume that the amplitudes a_k, phases ϕ_k, damping factors d_k, and frequencies f_k of the components within multiplets satisfy the following relations:

$$\begin{aligned} &a_k = c_k a \ (a = \text{unknown},\ c_k = \text{known real constants}),\\ &\phi_k = \phi \ (\phi = \text{unknown}),\\ &d_k = d \ (d = \text{unknown}),\\ &f_k = f + (k-1)\Delta f \ (f = \text{unknown},\ \Delta f = \text{known}), \end{aligned} \tag{1.2}$$

where k denotes the peak number in the considered multiplet components (e.g., doublet or triplet peaks) and Δf represents the frequency difference between the individual resonances within the considered multiplet.

In particular, the adenosine triphosphate complex, commonly called ATP, which has one triplet peak and two doublet peaks the parameters of which may in some cases be known to satisfy the above type of relations, will be considered as an example for the simulation and in vivo studies. The performance of KNOB-TLS will be compared, in terms of robustness and accuracy, with the subspace-based methods HTLS and HTLSPK(Δfd_{eq}), and with the interactive maximum-likelihood method AMARES [15]. A comparison in terms of computational efficiency is also carried out for the three aforementioned subspace-based methods. Our studies show that the proposed method performs much better than HTLS and HTLSPK (Δfd_{eq}) and provides parameter estimates comparable to the AMARES ones, but it is not able to outperform the interactive method in robustness and accuracy. However, AMARES is an optimization-based method which requires good initial parameter estimates to converge properly. Usually, the procedure used to obtain good starting values is the so-called "peak picking" procedure that involves a lot of interaction with the user. In this context, KNOB-TLS can be used to provide good starting values to AMARES, therefore decreasing the need for human interaction.

The paper is organized as follows. In Section 2 an outline of the KNOB-TLS algorithm is provided. In Section 3 the simulation studies are described and the performances of the four methods are compared in terms of robustness and accuracy. In Section 4 in vivo studies, using ^{31}P as well as proton MRS signals, are described and the performances of KNOB-TLS, HTLSPK(Δfd_{eq}), HTLS, and AMARES are compared in terms of accuracy. In Section 5 we formulate the main conclusions and, finally, in Appendix A the method KNOB-SVD/TLS is described.

2. KNOB-TLS algorithm for multiplet parameter estimation

We consider MRS signals characterized by one or more doublets and triplets. Without loss of generality, we focus on MRS signals with contribution from ATP, consisting of K components with $K \geqslant 7$, and containing

one triplet and two doublets. The dampings and frequencies of the triplet peak satisfy the following relations:

$$\begin{aligned} &d_1 = d_2 = d_3 = d_t, \\ &f_2 = f_1 + \Delta f, \quad f_3 = f_1 + 2\Delta f, \end{aligned} \tag{2.3}$$

the dampings and frequencies of the doublet peaks satisfy:

$$\begin{aligned} &d_4 = d_5 = d_{d1}, \quad f_5 = f_4 + \Delta f, \\ &d_6 = d_7 = d_{d2}, \quad f_7 = f_6 + \Delta f. \end{aligned} \tag{2.4}$$

Finally, the amplitudes and phases of the triplet and doublet peaks satisfy:

$$\begin{aligned} &2a_1 = a_2 = 2a_3 = a_4 = a_5 = a_6 = a_7 = a, \\ &\phi_1 = \phi_2 = \phi_3 = \phi_4 = \phi_5 = \phi_6 = \phi_7 = \phi, \end{aligned} \tag{2.5}$$

with d_t (damping for the triplet peak), d_{d1} (damping for the first doublet peak), d_{d2} (damping for the second doublet peak), a and ϕ unknown, and Δf known. We also assume, as prior knowledge, that the approximate frequency locations of the ATP peaks are known.

The KNOB-SVD/TLS method is briefly described in Appendix A. Here we summarize the computations required by KNOB-TLS.

2.1. Outline of the KNOB-TLS algorithm

- *Step 1*. Damping and frequency estimation of all peaks
  - Compute Λ defined in (A.4) using the HTLS method.
  - Extract Λ_2 and Λ_3 from the signal pole estimates in Λ.
- *Step 2*. Removal of nuisance peaks prior to triplet peak estimation
  - Use the estimates $\{\bar{\lambda}_1, \ldots, \bar{\lambda}_{\bar{m}}\} = \Lambda_3$, obtained in Step 1, to compute the QR decomposition in (A.7) and hence obtain $\bar{\mathbf{Q}}$.
  - Compute the $M \times (L - \bar{m})$ matrix $\bar{\mathbf{Y}}$, as in (A.9), from which the components outside the triplet region have been eliminated.
- *Step 3*. Damping and frequency estimation of the triplet peak
  - Compute the matrix $\bar{\mathbf{U}}$ consisting of the $\max\{K - \bar{m}, 3\}$ left singular vectors of $\bar{\mathbf{Y}}$ associated with the largest singular values.
  - Compute $\bar{\mathbf{\Gamma}}$ defined in (A.14) and its eigenvector $\mathbf{w}$ associated with the smallest eigenvalue.
  - Solve Eq. (A.21) in a TLS sense to obtain λ_1. Use the estimate of λ_1 along with (2.3) to estimate $\lambda_2 = \lambda_1 e^{j2\pi\Delta f \Delta t}$ and $\lambda_3 = \lambda_1 e^{j4\pi\Delta f \Delta t}$.
- *Step 4*. Removal of nuisance peaks prior to doublet peak estimation
  - Use the estimates $\{\breve{\lambda}_1, \ldots, \breve{\lambda}_{\breve{m}}\} = \Lambda_2$, obtained in Step 1, to compute a QR decomposition similar to (A.7) and hence obtain $\breve{\mathbf{Q}}$.
  - Compute the $M \times (L - \breve{m})$ matrix $\breve{\mathbf{Y}}$ from which the components outside the doublet regions have been eliminated.
- *Step 5*. Damping and frequency estimation of the doublet peaks
  - Compute the matrix $\breve{\mathbf{U}}$ consisting of the $\max\{K - \breve{m}, 4\}$ left singular vectors of $\breve{\mathbf{Y}}$ associated with the largest singular values.
  - Compute $\breve{\mathbf{\Gamma}}$ defined in (A.26) and its eigenvectors $\mathbf{w}_1, \mathbf{w}_2$ associated with the two smallest eigenvalues.
  - Solve Eq. (A.32) in a TLS sense to obtain the 2×2 matrix $\mathbf{\Psi}$ and take its two eigenvalues as estimates of λ_4 and λ_6. Use the estimates of λ_4 and λ_6 along with (2.4) to estimate $\lambda_5 = \lambda_4 e^{j2\pi\Delta f \Delta t}$ and $\lambda_7 = \lambda_6 e^{j2\pi\Delta f \Delta t}$.
- *Step 6*. Elimination of the estimated multiplet peaks
  - Use the estimates of $\{\lambda_k\}_{k=1}^{7}$, obtained in Steps 3 and 5, to compute a QR decomposition as in (A.7) and, hence, to compute the $M \times (L - 7)$ matrix $\mathbf{Y}_{K-7}$ from which the ATP peak components have been eliminated.
- *Step 7*. Damping and frequency estimation of the remaining $K - 7$ peaks
  - Similarly to Step 1, apply the HTLS method to the $K - 7$ dominant left singular vectors of the data matrix $\mathbf{Y}_{K-7}$ to re-estimate $\{\lambda_k\}_{k=8}^{K}$.
- *Step 8*. Amplitude estimation
  - Use the amplitude and phase constraints (2.5) into the model equation to obtain the system of linear equations $\mathbf{A\Theta} = \mathbf{y}$, as defined in (A.37), where $\mathbf{y}$ represents the data vector.
  - Compute the least-squares solution of the system $\mathbf{A\Theta} = \mathbf{y}$ in order to obtain the amplitude and phase estimates.

Remark. This algorithm can be easily adapted for quantitation of other signals with multiplet structure by combining, modifying and deleting the above steps in an appropriate way. For example, quantitation of a proton MRS signal exhibiting a lactate doublet involves the execution of Steps 1, 4 (restricted to one doublet), 5, 6, and 7 with proper specification of the amplitude and phase constraints.

3. Quantitation of a simulated MRS signal

We consider a simulated signal derived from an in vivo ^{31}P spectrum measured in the human brain and consisting of 256 complex data points and 11 exponentials, as defined in [15]. In Table 1 the parameters of the noiseless simulated signal are displayed and Fig. 1 shows the real part of the Discrete Fourier Transform (DFT) of the simulated signal when it is perturbed by additive complex white noise with a circular Gaussian distribution with standard deviation $\sigma = 15$. The first seven

Table 1
True parameter values of the simulated ^{31}P MRS signal

Peak k	f_k (Hz)	f_k (ppm)	d_k (Hz)	a_k (a.u.)	ϕ_k (°)
1	−86	−17.2	50	75	135
2	−70	−16.6	50	150	135
3	−54	−16.0	50	75	135
4	152	−8.0	50	150	135
5	168	−7.4	50	150	135
6	292	−2.6	50	150	135
7	308	−2.0	50	150	135
8	360	0.0	25	150	135
9	440	3.1	285.7	1400	135
10	490	5.0	25	60	135
11	530	6.6	200	500	135

peaks (denoted by β-ATP, α-ATP, and γ-ATP, respectively, in Fig. 1) represent the adenosine triphosphate (ATP) complex. We note that the ATP complex contains one triplet peak, β-ATP, and two doublet peaks, α-ATP and γ-ATP, which clearly satisfy the aforementioned properties (2.3)–(2.5). The β-ATP peak was approximated as a triplet in our in vivo examples. For highly resolved signals of tissues with known differences in the ATP phosphorus α–β and γ–β coupling constants, the β-ATP peak should be treated as a doublet of a doublet with the appropriate prior knowledge concerning the coupling constants, insofar available. The sampling frequency is $f_s = 3\,\text{kHz}$ and the frequency separation of the ATP peaks is $\Delta f = 16\,\text{Hz}$. In this section we compare the performances of the subspace-based methods KNOB-TLS, HTLS, HTLSPK($\Delta f d_{\text{eq}}$) and the optimization-based method AMARES when considering the full ^{31}P signal, whose first seven peaks, i.e., the ATP complex, satisfy the prior knowledge

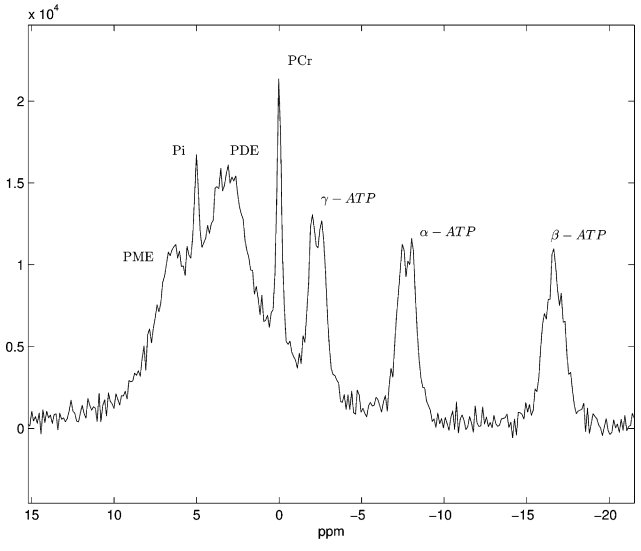

Fig. 1. Real part of the spectrum of the simulated ^{31}P MRS signal, obtained for $\sigma = 15$.

specified by the relations (2.3)–(2.5). Before describing the simulation studies, we would like to remind the reader that the method AMARES is initialized by using the "peak picking" technique, as already pointed out in Section 1. Moreover, it is important to note that the method HTLSPK($\Delta f d_{\text{eq}}$) can only exploit the type of prior knowledge considered in (1.2) for the doublet peaks, but not for triplet peaks. However, the method can be applied to the given signal by modeling the ATP triplet peak as two doublet peaks sharing the center peak. In the following, the method HTLSPK($\Delta f d_{\text{eq}}$) will be denoted by HTLSPK to simplify the notation.

We consider Eq. (1.1) with a_k, ϕ_k, d_k, and f_k, $k = 1, \ldots, 11$, as given in Table 1, and perturb the signal by adding white Gaussian noise with standard deviation σ on the real and the imaginary components separately. Our goal is to recover the parameters a_k, ϕ_k, d_k, and f_k, $k = 1, \ldots, 11$, characterizing the signal $\{y_n\}_{n=0}^{N-1}$, and compare the performances of KNOB-TLS, HTLS, HTLSPK, and AMARES in terms of robustness and statistical accuracy. The robustness of each method is evaluated by computing its success rate, i.e., the number of times, out of the total number of simulation runs, the method is able to resolve the 11 peaks within specific intervals lying symmetrically around the true frequencies of the peaks. The halfwidths of these intervals are set to 8 Hz, i.e., half the separation of the closest peaks in the data. Concerning the statistical accuracy, this is measured as the mean Relative Root Mean Squared Error (mean RRMSE)

$$\text{mean RRMSE} \equiv \frac{100}{K}\sum_{k=1}^{K}\sqrt{\frac{1}{J}\sum_{j=1}^{J}\frac{(\hat{p}_{k,j}-p_k)^2}{p_k^2}}(\%) \tag{3.6}$$

for the amplitude and damping estimates, and as the mean Root Mean Squared Error (mean RMSE)

$$\text{mean RMSE} \equiv \frac{1}{K}\sum_{k=1}^{K}\sqrt{\frac{1}{J}\sum_{j=1}^{J}(\hat{p}_{k,j}-p_k)^2} \tag{3.7}$$

for the frequency and phase estimates, where K is the total number of peaks ($K = 11$), J is the number of simulation runs in which the method was able to find every peak within the corresponding frequency interval, $\hat{p}_{k,j}$ denotes the parameter estimate of the kth peak obtained in simulation run j, and p_k denotes the true parameter value of the kth peak. We only take into account the results related to those cases for which we have a success rate of at least 5% (i.e., $J \geqslant 50$ when performing 1000 simulation runs), in order to prevent showing mean RRMSE and mean RMSE values which are based on too few estimates. In Fig. 2 the success rate and the amplitude mean RRMSE values for the ATP complex for different noise levels are displayed.

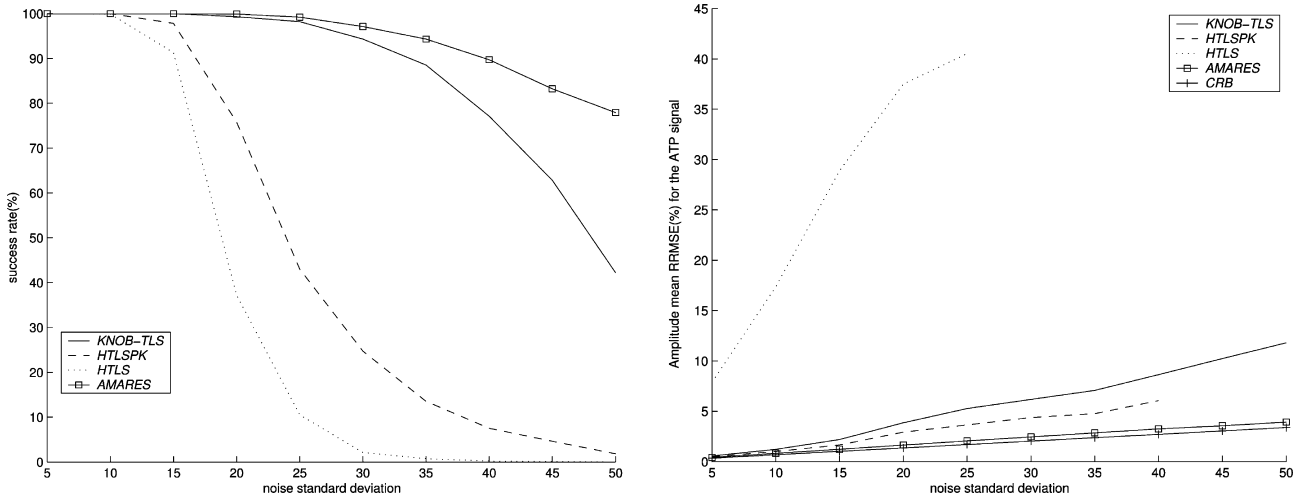

Fig. 2. Left: success rate as a function of the noise standard deviation σ for the ^{31}P signal. Right: mean RRMSE of amplitude estimates as a function of the noise standard deviation σ for the ATP complex.

We can observe that the method KNOB-TLS is much more robust than the other two subspace-based methods HTLS and HTLSPK, and it also provides amplitude estimates whose quality is much better than that of the HTLS estimates. Note that HTLSPK seems better than KNOB-TLS in accuracy, but this is due to the fact that only the successful runs (much fewer for HTLSPK) have been considered in the plot. Moreover, we can also observe that KNOB-TLS is not able to outperform the optimization-based method AMARES, whose success rate is the highest and whose mean RRMSEs more closely approach the CRBs, which represent the best possible accuracy that an unbiased estimator can achieve. In Figs. 3 and 4 the mean RMSE values for the frequency estimates, the mean RRMSE values for damping factor estimates, and the mean RMSE values for phase estimates are shown.

From Fig. 3 (left) we can notice that the frequency estimates are characterized by low mean RMSE values for all considered methods and that, in particular, KNOB-TLS is more accurate than HTLSPK and HTLS. Similar results can be observed for phases in Fig. 4, where we can also notice that the performance of the HTLS method gets even worse. Finally, in Fig. 3(right) we can see that KNOB-TLS and HTLSPK damping factor estimates are characterized by large variances (high mean RRMSEs) compared to AMARES, which points out a loss of accuracy for both methods when estimating the damping factors.

Concerning the computational efficiency, the average number of flops over 1000 simulation runs for the considered blackbox methods was computed for different lengths of the signal, as given by the number of data points N. The noise standard deviation was set to

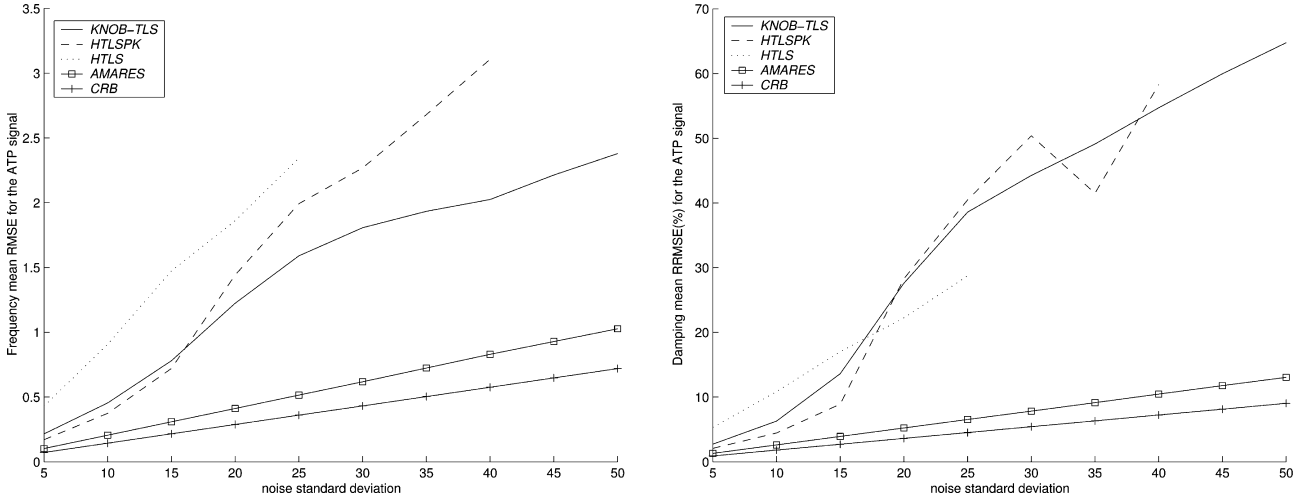

Fig. 3. Left: mean RMSE of frequency estimates as a function of the noise standard deviation σ for the ATP complex. Right: mean RRMSE of damping factor estimates as a function of the noise standard deviation σ for the ATP complex.

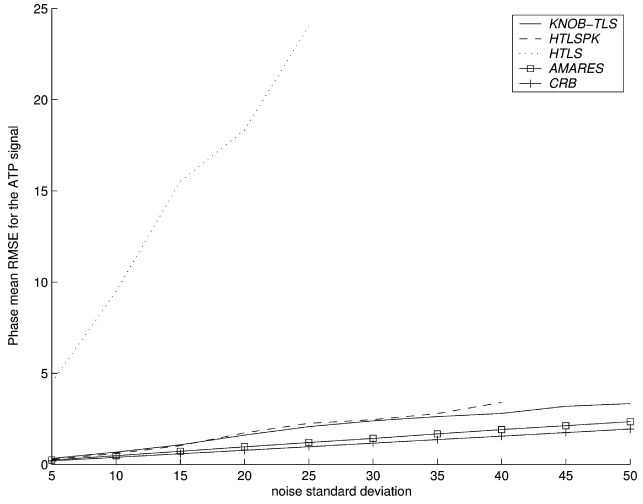

Fig. 4. Mean RMSE of phase estimates as a function of the noise standard deviation σ for the ATP complex.

$\sigma = 15$. The method AMARES has not been taken into account in the present comparison since the available code is written in Fortran, which does not allow the count of the number of flops. In Table 2 the ratio between the average number of flops of the two methods KNOB-TLS, HTLSPK, and the average number of flops of HTLS is reported. We observe that KNOB-TLS is about 1.5 times computationally more intensive than HTLSPK and that for all methods the ratio slightly increases with the length of the signal N. The efficiency of KNOB-TLS can be improved by using the Lanczos algorithm with partial reorthogonalization or the implicitly restarted Lanczos algorithm [17] in order to compute the truncated SVDs, which represent the computationally most intensive part of the algorithm.

Table 2
Ratio between the average number of flops over 1000 simulation runs for different lengths of the signal

N	(KNOB-TLS)/HTLS	HTLSPK/HTLS
256	9.3651	6.6832
1024	9.7731	6.8342
2048	9.7852	6.8491

We would like to conclude this section by describing the performance improvements which one can expect by using the TLS-based variant KNOB-TLS of the originally proposed method KNOB-SVD. We remind the reader that the difference between the two versions consists of computing the total-least squares solutions of Eq. (A.21) and (A.32) instead of the least-squares solutions. In Fig. 5 the amplitude (left) and damping (right) mean RRMSE values for the proposed method are reported when considering the two different variants: KNOB-SVD and KNOB-TLS. We can observe that the TLS variant provides amplitude and damping factor estimates whose quality is slightly better than that of the LS variant.

4. Quantitation of in vivo MRS signals

4.1. In vivo ^{31}P signals

As a first example of quantitation of in vivo MRS signals, we consider 21 ^{31}P signals, which are free-induction decay signals acquired after a single pulse (64 averages), obtained from the resting calf muscle of healthy humans and recorded at 81.1 MHz (4.7 T Bruker Biospec) using a 5 cm diameter surface coil positioned against the calf muscle. Each signal consists of 2048 complex data points in the time domain and is assumed to be modeled by Eq. (1.1) with model order $K = 9$. The sampling time is 0.25ms and only 512 data samples are

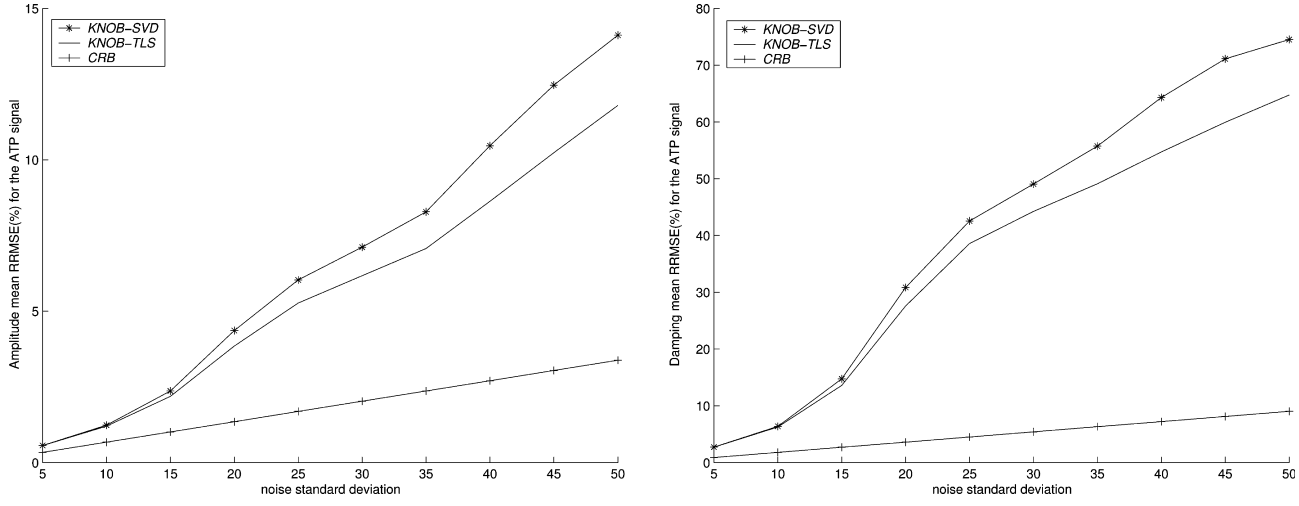

Fig. 5. Mean RRMSE of amplitude estimates (left) and damping estimates (right) as computed by KNOB-SVD and its TLS variant KNOB-TLS, as a function of the noise standard deviation σ for the ATP complex.

considered (the remaining ones contain only noise), starting from the 5th point of the signal (the first 4 data samples are excluded in order to eliminate the hump characterizing the original spectra). The same data samples are used in the KNOB-TLS, HTLSPK, HTLS, and AMARES estimation algorithms for the quantitation of the given signals. The method AMARES is initialized by using the "peak picking" technique applied to one of the available signals. The prior knowledge about amplitudes and phases we assume in this section slightly differs from (2.5) since the signals also contain the adenosine diphosphate complex, commonly called ADP, which distorts the original ATP signal. More precisely, we consider as prior knowledge for the β-ATP triplet peak

$$2a_1 = a_2 = 2a_3, \quad \phi_1 = \phi_2 = \phi_3 \tag{4.8}$$

for the first α-ATP doublet peak

$$a_4 = a_5, \quad \phi_4 = \phi_5, \tag{4.9}$$

and for the second γ-ATP doublet peak

$$a_6 = a_7, \quad \phi_6 = \phi_7. \tag{4.10}$$

Regarding the prior knowledge in (2.4) and (2.5), here Δf is equal to 16 Hz. The approximate frequency locations for all ATP peaks are known as well: β-ATP (−1129 Hz, −16.2 ppm; −1113 Hz, −16.0 ppm; −1097 Hz, −15.8 ppm), α-ATP (−426 Hz, −7.6 ppm; −410 Hz, −7.4 ppm), and γ-ATP (−20 Hz, −2.6 ppm; −4 Hz, −2.4 ppm). In order to compare the performances of various methods in terms of accuracy, we need the true parameter values which, unfortunately, are not known in practical applications. However, we can consider as accurate estimates of the true parameters those determined by AMARES. Our studies show that the parameter estimates provided by the method KNOB-TLS are the closest to the AMARES estimates. More precisely, the method KNOB-TLS is always able to resolve correctly the first 8 peaks (β-ATP, α-ATP, γ-ATP, and PCr), but not always the 9th one (Pi), the reason being that the Pi peak was almost inexistent in some of the spectra, while prominent in others, reflecting the biological variation of the concentration of muscle Pi in individuals. The methods HTLSPK and HTLS are not able to provide acceptable estimates, that is their frequency estimates do not fall within the frequency intervals lying symmetrically around the AMARES estimates and with halfwidths equal to 8 Hz. The method HTLSPK is sometimes able to resolve the α-ATP and γ-ATP doublets and the PCr peak, but never the β-ATP triplet and the Pi peak; HTLS never resolves the triplet and doublets. Fig. 6 shows results of quantifying one of the available ^{31}P MRS signals by AMARES and KNOB-TLS. In Table 3 the mean Relative Root Mean Square Difference values (mean RRMSD) for the amplitude and the damping parameter estimates, and the mean Root Mean Square Difference (mean RMSD) values for the frequency and phase parameter estimates are reported. They are obtained for the ATP triplet and doublets by processing the available 21 signals. The formulas used to compute the mean RRMSDs and the mean RMSDs are respectively:

$$\text{mean RRMSD} \equiv \frac{100}{K}\sum_{k=1}^{K}\sqrt{\frac{1}{J}\sum_{j=1}^{J}\frac{(\hat{p}_{k,j}-p_{k,j})^2}{p_{k,j}^2}}(\%) \tag{4.11}$$

and

$$\text{mean RMSD} \equiv \frac{1}{K}\sum_{k=1}^{K}\sqrt{\frac{1}{J}\sum_{j=1}^{J}(\hat{p}_{k,j}-p_{k,j})^2}, \tag{4.12}$$

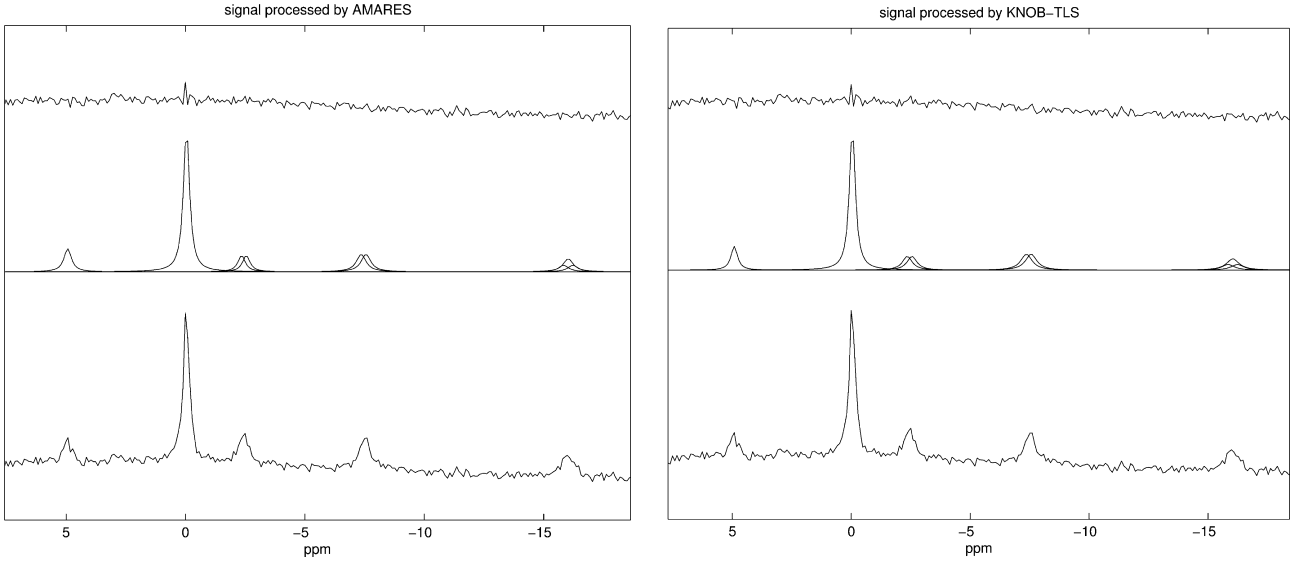

Fig. 6. Real part of the original ^{31}P signal spectrum (bottom); (middle) real part of the spectra of the individual peaks estimated by AMARES (left) and KNOB-TLS (right); (top) real part of the residual signal spectrum after estimation with AMARES (left) and KNOB-TLS (right).

Table 3
Mean RMSD (RRMSD) values and minimum and maximum difference (relative difference) values of the frequency and phase (amplitude and damping) estimates for in vivo ^{31}P MRS signals measured from the calf muscle of healthy humans

Peak	Method	f_k mean RMSD [m,M]	d_k mean RRMSD [m,M] (%)	a_k mean RRMSD [m,M] (%)	ϕ_k mean RMSD [m,M]
β-ATP	KNOB-TLS	0.64 [0.03,1.45]	33.91 [20.49,50.73]	16.52 [9.13,23.07]	1.23 [0.09,2.67]
	HTLSPK	323.66 [5.65,393.28]	23.94 [8.23,34.11]	72.81 [8.57,99.26]	126.69 [8.88,169.75]
	HTLS	529.61 [0.07,1085.31]	60.46 [3.14,111.98]	213.51 [87.62,460.38]	66.08 [0.02,207.52]
α-ATP	KNOB-TLS	0.75 [0.02,1.55]	15.58 [8.10,27.13]	8.68 [2.33,13.49]	2.34 [0.02,4.66]
	HTLSPK	346.85 [6.81,424.20]	12.73 [2.24,30.36]	19.47 [0.33,50.09]	15.87 [0.38,39.90]
	HTLS	307.15 [6.52,612.93]	36.59 [0.13,101.09]	185.51 [10.24,555.47]	39.72 [0.11,210.73]
γ-ATP	KNOB-TLS	2.48 [0.12,6.05]	51.38 [5.01,91.78]	27.98 [3.52,54.47]	5.93 [0.19,12.60]
	HTLSPK	908.64 [2.80,1710.04]	449.61 [15.60,1892.90]	118.74 [23.20,413.71]	97.32 [5.20,231.77]
	HTLS	278.85 [179.38,590.50]	55.42 [2.01,103.32]	344.52 [6.42,799.84]	41.12 [0.11,163.09]

where K is the number of peaks, J is the total number of processed in vivo signals ($J = 21$), $\hat{p}_{k,j}$ denotes the parameter estimate of the kth peak obtained when processing the jth signal by one of the blackbox methods, and $p_{k,j}$ denotes the AMARES parameter estimate of the kth peak for the jth signal. The table also reports the minimum (m) and maximum (M) relative difference values (for the amplitude and the damping estimates) and the minimum (m) and maximum (M) difference values (for the frequency and phase estimates) for each method. It is observed that KNOB-TLS is much more accurate than HTLSPK and HTLS: its mean RRMSD and mean RMSD values are generally the smallest.

4.2. In vivo proton signals

As a second example of quantitation of in vivo MRS signals, we consider a long echo-time proton signal from a 7.5 cm^3 volume in the white matter of the brain of a 3.5 years old child with leukodystrophy, acquired at 63.6 MHz on a 1.5 T Siemens Sonata scanner using the STEAM sequence (TR/TE/TM = 2000/135/30 ms) and CHESS water suppression. The data consist of 1024 complex points in the time domain and the sampling time is 1 ms. Only 512 data points are considered in the analysis (the remaining ones contain only noise) starting from the 2nd one (the first one is excluded to eliminate the hump characterizing the original spectrum). The signal is characterized by the presence of the following compounds: inverted lactate doublet (Lac), *N*-acetyl aspartate (NAA), creatine (Cr), choline (Cho), and the water resonance whose magnitude, as is well-known, is much larger than the magnitude of the metabolites of interest. The available prior knowledge is related to the lactate doublet with Δf known and equal to 7 Hz. The approximate frequency locations for all peaks of interest are known as well: Lac (−215 Hz, 1.3 ppm; −208 Hz, 1.4 ppm), NAA (−169 Hz, 2.1 ppm), Cr (−104 Hz, 3.1 ppm), and Cho (−92 Hz, 3.3 ppm). The choice of the model order K, which characterizes Eq. (1.1), represents an important step since we have to take into account the contribution of the residual water signal: a too small value of K could result in information loss, while a too large value could incorporate too much noise and generate spurious spectral features. Several criteria, which estimate the model order when unknown, are available in the literature. We chose to apply the minimum description length (MDL) criterion [18,19], which estimates the best model order by minimizing a discrete function of the singular values of the Hankel matrix (A.1). We obtained the value $K = 7$, which means that the residual water resonance is modeled by two exponentially damped complex sinusoids. In Table 4 the parameter estimates obtained when processing the signal by AMARES (after water removal by HSVD) and the three blackbox methods are displayed. Notice that the methods KNOB-TLS and HTLSPK provide estimates which are very close to the AMARES ones. However, KNOB-TLS is more accurate than HTLSPK. In the present case, also HTLS seems to provide acceptable parameter estimates, but it is important to note that the imposed prior knowledge concerning the lactate doublet is not satisfied, especially for the damping factor, amplitude, and phase estimates. Fig. 7 shows the results of the quantitation of the proton MRS signal for AMARES and KNOB-TLS. Similar results are obtained when quantifying other in vivo proton MRS signals.

5. Conclusions

In this paper a new subspace-based parameter estimation method, called KNOB-SVD, and its TLS variant KNOB-TLS have been described. They are able to exploit biochemical prior knowledge, which is often available when considering MRS signals and whose use is important for accuracy and resolution. The performance of the proposed method has been compared, in terms of robustness and accuracy, to that of three well known estimation methods: the interactive method AMARES and the two blackbox methods HTLS and HTLSPK($\Delta f d_{eq}$). Our extensive simulation and in vivo studies show that, in general, the inclusion of prior knowledge in estimation algorithms improves both robustness and accuracy of the parameter estimates. Indeed, the methods KNOB-SVD/

Table 4
Parameter estimates and their CRBs for an in vivo proton MRS signal measured from the human brain

Peak	Method	f_k (Hz)	d_k (Hz)	a_k (a.u.)	ϕ_k (°)
1	AMARES	-215.22 ± 0.08	4.97 ± 0.52	13.90 ± 0.96	55.07 ± 0.07
Lac (−215 Hz)	KNOB-TLS	-214.97 ± 0.08	4.87 ± 0.52	13.62 ± 0.96	65.77 ± 0.07
	HTLSPK	-215.02 ± 0.10	6.32 ± 0.63	15.31 ± 1.03	63.29 ± 0.07
	HTLS	-215.04 ± 0.08	2.94 ± 0.52	8.71 ± 1.03	57.71 ± 0.06
2	AMARES	-208.22 ± 0.08	4.97 ± 0.52	13.90 ± 0.96	55.07 ± 0.07
Lac (−208 Hz)	KNOB-TLS	-207.97 ± 0.08	4.87 ± 0.52	13.62 ± 0.96	65.77 ± 0.07
	HTLSPK	-208.02 ± 0.10	6.32 ± 0.63	15.31 ± 1.03	63.29 ± 0.07
	HTLS	-208.07 ± 0.08	6.38 ± 0.52	18.53 ± 1.03	73.59 ± 0.06
3	AMARES	-168.09 ± 0.16	7.80 ± 1.01	19.40 ± 1.80	-124.93 ± 0.09
NAA	KNOB-TLS	-168.36 ± 0.16	7.75 ± 1.01	19.12 ± 1.79	-137.65 ± 0.09
	HTLSPK	-168.34 ± 0.16	7.66 ± 1.01	18.92 ± 1.78	-136.63 ± 0.09
	HTLS	-168.34 ± 0.16	7.58 ± 0.99	18.84 ± 1.77	-137.37 ± 0.09
4	AMARES	-103.62 ± 0.19	8.91 ± 1.19	21.02 ± 2.15	-124.93 ± 0.10
Cr	KNOB-TLS	-103.13 ± 0.18	8.65 ± 1.15	20.93 ± 2.13	-108.78 ± 0.10
	HTLSPK	-103.13 ± 0.18	8.58 ± 1.15	20.75 ± 2.12	-108.57 ± 0.10
	HTLS	-103.13 ± 0.18	8.50 ± 1.14	20.71 ± 2.11	-108.83 ± 0.10
5	AMARES	-92.00 ± 0.10	9.35 ± 0.61	44.09 ± 2.20	-124.93 ± 0.05
Cho	KNOB-TLS	-92.02 ± 0.10	9.52 ± 0.61	45.79 ± 2.24	-126.79 ± 0.05
	HTLSPK	-92.02 ± 0.10	9.49 ± 0.61	45.67 ± 2.24	-126.59 ± 0.05
	HTLS	-92.01 ± 0.10	9.48 ± 0.60	45.69 ± 2.23	-126.62 ± 0.05

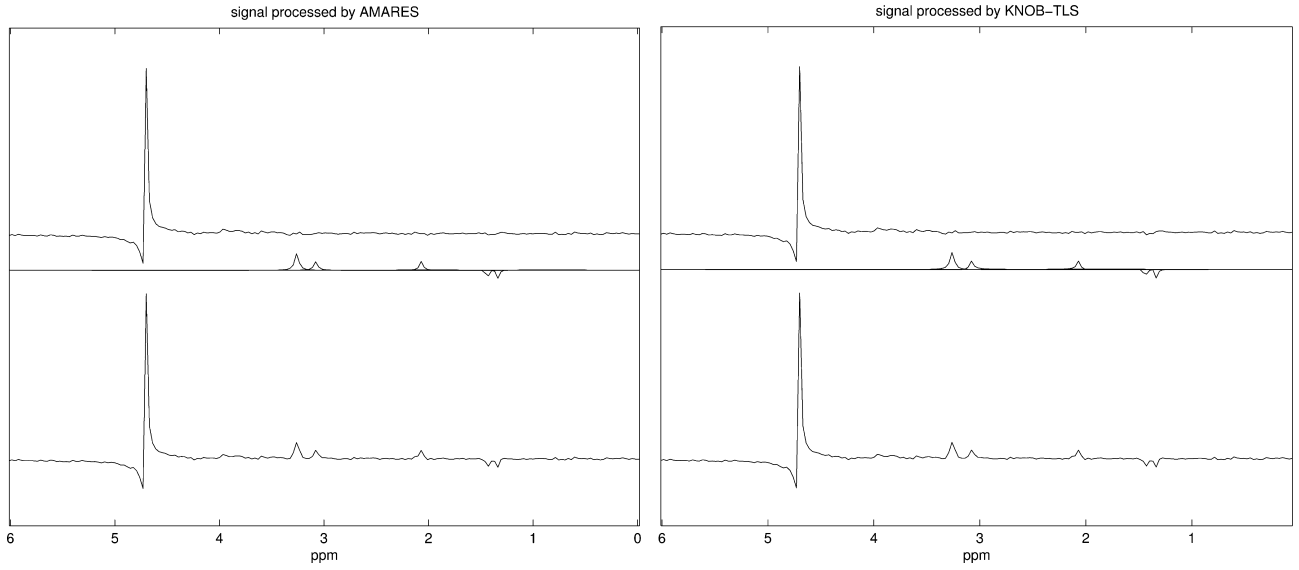

Fig. 7. Real part of the original proton signal spectrum (bottom); (middle) real part of the spectra of the individual peaks estimated by AMARES (left) and KNOB-TLS (right); (top) real part of the residual signal spectrum after estimation with AMARES (left) and KNOB-TLS (right).

TLS, HTLSPK(Δfd_{eq}), and AMARES outperform the method HTLS which does not allow the inclusion of any prior knowledge. Moreover, KNOB-SVD/TLS is able to outperform the method HTLSPK(Δfd_{eq}), especially in terms of robustness, and to provide parameter estimates which are comparable to the AMARES ones. However, it is not able to outperform the interactive method AMARES, which is the most robust and accurate method.

Since AMARES is an optimization-based method which requires good initial parameter estimates to converge properly, the proposed method KNOB-SVD/TLS can be used to provide good starting values to the interactive AMARES method, hence decreasing the need for human interaction.

Acknowledgments

Research supported by Research Council KUL: GOA-Mefisto 666, IDO /99/003 and IDO /02/009 (Predictive computer models for medical classification

problems using patient data and expert knowledge), several PhD/postdoc and fellow grants; Flemish Government: FWO: PhD/postdoc grants, projects, G.0200.00 (damage detection in composites by optical fibres), G.0078.01 (structured matrices), G.0407.02 (support vector machines), G.0269.02 (magnetic resonance spectroscopic imaging), G.0270.02 (nonlinear Lp approximation), research communities (ICCoS, ANMMM); IWT: PhD Grants, Belgian Federal Government: DWTC (IUAP IV-02 (1996-2001) and IUAP V-22 (2002-2006): Dynamical Systems and Control: Computation, Identification, and Modelling); EU: NICONET, INTERPRET, PDT-COIL, MRS/MRI signal processing (TMR). The research of P. Stoica and Y. Selén was partly supported by the Swedish Science Council (VR).

Appendix A. The KNOB-SVD/TLS algorithm

The algorithm KNOB-SVD has been described in [14] but is repeated here for clarity of exposition.

As already indicated in Section 2, we consider MRS signals characterized by one or more doublets and triplets. Without loss of generality, we focus on MRS signals with contribution from ATP, consisting of K components with $K \geqslant 7$, and containing one triplet and two doublets. We assume as prior knowledge the relations (2.3)–(2.5). The KNOB-SVD/TLS method is described in the following steps:

- *Step* 1. Damping and frequency estimation of all peaks

  Let $\mathbf{Y}$ denote the Hankel data matrix commonly used in SVD-based parameter estimation methods

$$\mathbf{Y} = \begin{bmatrix} y_0 & y_1 & \cdots & y_{N-M} \\ \vdots & \vdots & \vdots & \vdots \\ y_{M-1} & y_M & \cdots & y_{N-1} \end{bmatrix}, \tag{A.1}$$

  where M is a user parameter usually chosen less than but close to $N/2$ in order to get the best possible parameter estimation accuracy [10,12,16]. We suggest the value $M = 2N/5$.

  For a noiseless signal, i.e., $\epsilon_n = 0$ in (1.1), the matrix $\mathbf{Y}$ can be written as:

$$\mathbf{Y} = [\mathbf{a}_M(\lambda_1) \ldots \mathbf{a}_M(\lambda_K)], \tag{A.2}$$

$$\begin{bmatrix} a_1 e^{j\phi_1} & & 0 \\ & \ddots & \\ 0 & & a_K e^{j\phi_K} \end{bmatrix} \begin{bmatrix} \mathbf{a}_L^T(\lambda_1) \\ \vdots \\ \mathbf{a}_L^T(\lambda_K) \end{bmatrix},$$

  where $L = N - M + 1$ and for $P = M$, L or N

$$\mathbf{a}_P(\lambda) = \begin{bmatrix} 1 & \lambda & \cdots & \lambda^{P-1} \end{bmatrix}^{\mathrm{T}}. \tag{A.3}$$

  We apply a standard subspace-based method, like HSVD/HTLS, to the K dominant left singular vectors of the data matrix $\mathbf{Y}$ to compute the set of signal poles

$$\Lambda = \{\lambda_1, \ldots, \lambda_K\} \tag{A.4}$$

  related to the K signal components. Since we know the approximate frequency locations for the triplet and the two doublets, we can identify which ones of the estimated signal poles correspond to the triplet peak and which ones to the doublet peaks. Then, we can define the following subsets of Λ:

$$\Lambda_2 = \Lambda - \{\text{the doublet peaks } \{\lambda_k\}\}, \tag{A.5}$$

$$\Lambda_3 = \Lambda - \{\text{the triplet peak } \{\lambda_k\}\}, \tag{A.6}$$

  where the set Λ_2 contains the λ_k estimates with frequencies not close to any of the considered doublet peaks and Λ_3 contains the λ_k estimates with frequencies not close to the triplet peak.

- *Step* 2. Removal of nuisance peaks prior to triplet peak estimation

  Before estimating the triplet peak parameters, we have to eliminate the components corresponding to other peaks from the data which may disturb the triplet peak estimation. Actually, this might be unnecessary for low noise levels provided there are no other triplet peaks in the data satisfying (2.3). However, for higher noise levels, large peaks in the data may disturb the triplet peak estimation and, therefore, we first eliminate the non-triplet components in Λ_3 from the data matrix by using the technique described in [10]. Specifically, we assume that Λ_3 contains $\bar{m}$ elements, i.e., $\Lambda_3 = \{\bar{\lambda}_1, \ldots, \bar{\lambda}_{\bar{m}}\}$, and consider the QR decomposition of the following matrix:

$$\begin{bmatrix} \mathbf{a}_L(\bar{\lambda}_1) & \cdots & \mathbf{a}_L(\bar{\lambda}_{\bar{m}}) \end{bmatrix} = \begin{bmatrix} \bar{\mathbf{X}} & \bar{\mathbf{Q}} \end{bmatrix} \begin{bmatrix} \bar{\mathbf{R}} \\ \mathbf{0} \end{bmatrix}, \tag{A.7}$$

  where $\bar{\mathbf{X}}$, $\bar{\mathbf{Q}}$, and $\bar{\mathbf{R}}$ have dimensions $L \times \bar{m}$, $L \times (L - \bar{m})$, $\bar{m} \times \bar{m}$ respectively, $\bar{\mathbf{Q}}^* \bar{\mathbf{Q}} = \mathbf{I}_{L-\bar{m}}$ and $*$ denotes the conjugate transpose.

  As $\bar{\mathbf{Q}}^* \bar{\mathbf{X}} = \mathbf{0}$ by definition, we have

$$\bar{\mathbf{Q}}^* \mathbf{a}_L(\lambda) = \mathbf{0} \quad \text{for } \lambda = \bar{\lambda}_1, \ldots, \bar{\lambda}_{\bar{m}}, \tag{A.8}$$

  which implies that

$$\bar{\mathbf{Y}} \triangleq \mathbf{Y} \bar{\mathbf{Q}}^{*T} = \begin{bmatrix} \mathbf{a}_M(\check{\lambda}_1) & \ldots & \mathbf{a}_M(\check{\lambda}_{K-\bar{m}}) \end{bmatrix}, \tag{A.9}$$

$$\begin{bmatrix} \check{a}_1 e^{j\check{\phi}_1} & & \mathbf{0} \\ & \ddots & \\ \mathbf{0} & & \check{a}_{K-\bar{m}} e^{j\check{\phi}_{K-\bar{m}}} \end{bmatrix} \begin{bmatrix} \mathbf{a}_L^T(\check{\lambda}_1) \bar{\mathbf{Q}}^{*T} \\ \vdots \\ \mathbf{a}_L^T(\check{\lambda}_{K-\bar{m}}) \bar{\mathbf{Q}}^{*T} \end{bmatrix},$$

  where $\{\check{\lambda}_1, \ldots, \check{\lambda}_{K-\bar{m}}\} = \Lambda - \Lambda_3$. The matrix $\bar{\mathbf{Y}}$ no longer contains the components in Λ_3, i.e., $\bar{\mathbf{Y}}$ only contains the components corresponding to the triplet peak and, possibly, other peaks that are very close to the triplet peak.

- *Step* 3. Damping and frequency estimation of the triplet peak
  We compute the SVD of the matrix $\bar{\mathbf{Y}}$

$$\bar{\mathbf{Y}} = \bar{\mathbf{U}}\bar{\mathbf{\Sigma}}\bar{\mathbf{V}}^*, \tag{A.10}$$

where $\bar{\mathbf{\Sigma}} = \mathrm{diag}(\bar{\sigma}_1, \cdots, \bar{\sigma}_{K-\bar{m}})$, $\bar{\mathbf{U}}^*\bar{\mathbf{U}} = \mathbf{I}_{K-\bar{m}}$, and $\bar{\mathbf{V}}^*\bar{\mathbf{V}} = \mathbf{I}_{K-\bar{m}}$. We define the orthogonal projection matrix onto the nullspace of $\bar{\mathbf{U}}^*$

$$\bar{\mathbf{\Pi}} = \mathbf{I} - \bar{\mathbf{U}}\bar{\mathbf{U}}^*. \tag{A.11}$$

It is well known that the vectors $\{\mathbf{a}_M(\check{\lambda}_k)\}_{k=1}^{K-\bar{m}}$ span the range space of $\bar{\mathbf{U}}$ (see e.g. [16]) and hence

$$\sum_{k=1}^{K-\bar{m}} \mathbf{a}_M^*(\check{\lambda}_k)\bar{\mathbf{\Pi}}\mathbf{a}_M(\check{\lambda}_k) = 0. \tag{A.12}$$

Since for the noise-free case $\{\lambda_1, \lambda_2, \lambda_3\} \subset \{\check{\lambda}_1, \ldots, \check{\lambda}_{K-\bar{m}}\}$, where $\{\lambda_1, \lambda_2, \lambda_3\}$ are the signal poles associated with the triplet peak, we have

$$\sum_{k=1}^{3} \mathbf{a}_M^*(\lambda_k)\bar{\mathbf{\Pi}}\mathbf{a}_M(\lambda_k) = 0. \tag{A.13}$$

Let

$$\bar{\mathbf{\Gamma}} = \bar{\mathbf{\Pi}} + \mathbf{D}\bar{\mathbf{\Pi}}\mathbf{D}^* + \mathbf{D}^2\bar{\mathbf{\Pi}}\mathbf{D}^{*2}, \tag{A.14}$$

where $\mathbf{D}$ is defined as follows:

$$\mathbf{D} = \mathrm{diag}\left(1, \mathrm{e}^{-j2\pi\Delta f\Delta t}, \ldots, \mathrm{e}^{-j(M-1)2\pi\Delta f\Delta t}\right). \tag{A.15}$$

As

$$\mathbf{a}_M(\lambda_2) = \mathbf{D}^*\mathbf{a}_M(\lambda_1), \quad \mathbf{a}_M(\lambda_3) = \mathbf{D}^{*2}\mathbf{a}_M(\lambda_1),$$

it follows from (A.13) that

$$\mathbf{a}_M(\lambda_1) \in \mathrm{nullspace}(\bar{\mathbf{\Gamma}}), \tag{A.16}$$

and it can be shown that

$$\dim[\mathrm{nullspace}(\bar{\mathbf{\Gamma}})] = 1. \tag{A.17}$$

Let $\mathbf{w}$ denote the $M \times 1$ vector which spans the null space of $\bar{\mathbf{\Gamma}}$. In view of (A.16) and (A.17), we have that

$$\mathbf{a}_M(\lambda_1) = \rho\mathbf{w} \tag{A.18}$$

for some scalar $\rho \neq 0$. We define the following subvectors of $\mathbf{a}_M(\lambda)$

$$\mathbf{a}_u(\lambda) = [\,\mathbf{I}_{M-1} \quad \mathbf{0}\,]\mathbf{a}_M(\lambda), \tag{A.19}$$

$$\mathbf{a}_l(\lambda) = [\,\mathbf{0} \quad \mathbf{I}_{M-1}\,]\mathbf{a}_M(\lambda), \tag{A.20}$$

and similarly for $\mathbf{w}$. As $\mathbf{a}_l(\lambda) = \lambda\mathbf{a}_u(\lambda)$, we derive from (A.18) that

$$\rho\mathbf{w}_l = \lambda_1\rho\mathbf{w}_u \iff \mathbf{w}_l = \lambda_1\mathbf{w}_u \tag{A.21}$$

and hence λ_1 can be obtained as

$$\lambda_1 = \frac{\mathbf{w}_u^*\mathbf{w}_l}{\mathbf{w}_u^*\mathbf{w}_u}. \tag{A.22}$$

For noisy data, we compute the matrix $\bar{\mathbf{U}}$ made from the $\max\{K - \bar{m}, 3\}$ left singular vectors of $\bar{\mathbf{Y}}$ associated with the largest singular values. The vector $\mathbf{w}$ is the eigenvector of the matrix $\bar{\mathbf{\Gamma}}$ associated with the smallest eigenvalue. We use the estimate λ_1 along with Eq. (2.3) to estimate $\lambda_2 = \lambda_1\mathrm{e}^{j2\pi\Delta f\Delta t}$ and $\lambda_3 = \lambda_1\mathrm{e}^{j4\pi\Delta f\Delta t}$.

Note that the above value λ_1 was computed as the least-squares solution of Eq. (A.21). It is possible to solve Eq. (A.21) in the total least-squares sense [8], which results in more accurate final parameter estimates. For clarity of exposition, we show here how to compute λ_1 as the TLS solution of Eq. (A.21):

- arrange the vectors $\mathbf{w}_l$ and $\mathbf{w}_u$ in matrix form:

$$[\mathbf{w}_u, \mathbf{w}_l],$$

- compute the SVD of the matrix $[\mathbf{w}_u, \mathbf{w}_l]$:

$$[\mathbf{w}_u, \mathbf{w}_l] = \mathbf{U}_\mathbf{w}\mathbf{\Sigma}_\mathbf{w}\mathbf{V}_\mathbf{w}^*,$$

where $\mathbf{V}_\mathbf{w}$ has dimension 2×2

- TLS solution:

$$\lambda_1 = \frac{-\mathbf{V}_\mathbf{w}(1,2)}{\mathbf{V}_\mathbf{w}(2,2)},$$

where we used the Matlab notation to denote the $\mathbf{V}_\mathbf{w}$ matrix elements.

Using TLS instead of LS, as above, we obtain a variant of the KNOB-SVD method, called KNOB-TLS, which has been used in Sections 3 and 4 for the simulation and in vivo studies.

- *Step* 4. Removal of nuisance peaks prior to doublet peak estimation
  Before estimating the doublet peaks, we need to eliminate the triplet peak from the data since, in the theoretical development of the step dealing with the doublet peaks, we assume that there is no other doublet peak in the signal spectrum with the same damping and frequency separation. This assumption would be violated if the triplet peak was not eliminated. Also, for the noisy case, non-doublet peaks might disturb the estimation of the doublet peaks and, therefore, we want to eliminate those peaks as well. To eliminate the nuisance components from the data matrix $\mathbf{Y}$ prior to the doublet peak estimation, we use the same technique as for Step 2, but we replace Λ_3 by Λ_2 and we let $\breve{\mathbf{Y}}$ denote the output matrix.
- *Step* 5. Damping and frequency estimation of the doublet peaks
  We consider the SVD of the matrix $\breve{\mathbf{Y}}$ provided by the previous step

$$\breve{\mathbf{Y}} = \breve{\mathbf{U}}\breve{\mathbf{\Sigma}}\breve{\mathbf{V}}^*, \tag{A.23}$$

where $\breve{\mathbf{\Sigma}} = \mathrm{diag}(\breve{\sigma}_1, \ldots, \breve{\sigma}_{K-\breve{m}})$, $\breve{\mathbf{U}}^*\breve{\mathbf{U}} = \mathbf{I}_{K-\breve{m}}$ and $\breve{\mathbf{V}}^*\breve{\mathbf{V}} = \mathbf{I}_{K-\breve{m}}$, and $\breve{m}$ represents the number of elements in Λ_2. Let

$$\breve{\mathbf{\Pi}} = \mathbf{I} - \breve{\mathbf{U}}\breve{\mathbf{U}}^*. \tag{A.24}$$

A procedure similar to (A.13)–(A.16) shows that for the noise free case

$$\mathbf{a}_M(\lambda_4), \mathbf{a}_M(\lambda_6) \in \text{nullspace}(\breve{\mathbf{\Gamma}}), \tag{A.25}$$

where

$$\breve{\mathbf{\Gamma}} = \breve{\mathbf{\Pi}} + \mathbf{D}\breve{\mathbf{\Pi}}\mathbf{D}^*, \tag{A.26}$$

with

$$\dim[\text{nullspace}(\breve{\mathbf{\Gamma}})] = 2. \tag{A.27}$$

Let $\{\mathbf{w}_1, \mathbf{w}_2\}$ denote the $M \times 1$ vectors that span the null space of $\breve{\mathbf{\Gamma}}$. In view of (A.25), we have that

$$\begin{bmatrix} \mathbf{a}_M(\lambda_4) & \mathbf{a}_M(\lambda_6) \end{bmatrix} = \mathbf{WP}, \tag{A.28}$$

where $\mathbf{P}$ is a 2×2 non-singular matrix and

$$\mathbf{W} = \begin{bmatrix} \mathbf{w}_1 & \mathbf{w}_2 \end{bmatrix}. \tag{A.29}$$

We define

$$\mathbf{W}_u = [\mathbf{I}_{M-1} \quad \mathbf{0}]\mathbf{W}, \tag{A.30}$$

$$\mathbf{W}_l = [\mathbf{0} \quad \mathbf{I}_{M-1}]\mathbf{W}. \tag{A.31}$$

Then, it follows from (A.28) that

$$\mathbf{W}_l\mathbf{P} = \mathbf{W}_u\mathbf{P}\begin{bmatrix} \lambda_4 & 0 \\ 0 & \lambda_6 \end{bmatrix} \iff \mathbf{W}_l = \mathbf{W}_u\mathbf{\Psi}, \tag{A.32}$$

where

$$\mathbf{\Psi} = \mathbf{P}\begin{bmatrix} \lambda_4 & 0 \\ 0 & \lambda_6 \end{bmatrix}\mathbf{P}^{-1}. \tag{A.33}$$

We can obtain $\mathbf{\Psi}$ from (A.32) as follows:

$$\mathbf{\Psi} = (\mathbf{W}_u^*\mathbf{W}_u)^{-1}\mathbf{W}_u^*\mathbf{W}_l, \tag{A.34}$$

and, then, obtain λ_4 and λ_6 as the eigenvalues of $\mathbf{\Psi}$. As in Step 3, we can solve Eq. (A.32) in the TLS sense:

- arrange the matrices $\mathbf{W}_l$ and $\mathbf{W}_u$ in a new matrix: $[\mathbf{W}_u, \mathbf{W}_l]$,
- compute the SVD of the matrix $[\mathbf{W}_u, \mathbf{W}_l]$: $[\mathbf{W}_u, \mathbf{W}_l] = \mathbf{U}_\mathbf{W}\mathbf{\Sigma}_\mathbf{W}\mathbf{V}_\mathbf{W}^*$, where $\mathbf{V}_\mathbf{W}$ has dimension 4×4,
- TLS solution: $\mathbf{\Psi} = -\mathbf{V}_\mathbf{W}(1:2, 3:4)(\mathbf{V}_\mathbf{W}(3:4, 3:4))^{-1}$, where we used the Matlab notation to denote the $\mathbf{V}_\mathbf{W}$ matrix blocks.

For noisy data we compute the matrix $\breve{\mathbf{U}}$ made from the $max\{K - \breve{m}, 4\}$ left singular vectors of $\breve{\mathbf{Y}}$ associated with the largest singular values. The vectors $\{\mathbf{w}_1, \mathbf{w}_2\}$ are the eigenvectors of the matrix $\breve{\mathbf{\Gamma}}$ associated with the smallest eigenvalues. We use the estimates of λ_4 and λ_6 along with (2.4) to estimate $\lambda_5 = \lambda_4 e^{j2\pi\Delta f\Delta t}$ and $\lambda_7 = \lambda_6 e^{j2\pi\Delta f\Delta t}$.

- *Step* 6. Elimination of the estimated multiplet peaks

As already specified, the signal we are considering may contain other peaks besides the seven ATP peaks (the triplet and two doublets) we have already estimated. In order to improve the estimation of the remaining $K - 7$ peaks, we eliminate the 7 estimated peaks from the original data matrix $\mathbf{Y}$ and re-estimate the parameters of the remaining peaks.

Once again we apply the same technique used in Step 2 by replacing Λ_3 with

$$\Lambda_{\text{known}} = \{\lambda_1, \ldots, \lambda_7\} \tag{A.35}$$

and denoting the output data matrix as $\mathbf{Y}_{K-7}$.

- *Step* 7. Damping and frequency estimation of the remaining $K - 7$ peaks

Similarly to Step 1, we apply a standard HSVD/HTLS method to the $K - 7$ dominant left singular vectors of the data matrix $\mathbf{Y}_{K-7}$ to re-estimate $\{\lambda_8, \ldots, \lambda_K\}$.

- *Step* 8. Amplitude estimation

Once the signal poles $\{\lambda_k\}_{k=1}^K$ have been estimated, we can compute the amplitude estimates. Let

$$\mathbf{y} = \begin{bmatrix} y_0 & \cdots & y_{N-1} \end{bmatrix}^{\mathrm{T}} \tag{A.36}$$

denote the data vector.

By using the amplitude and phase constraints (2.5) into the model equation, we obtain (in the noise-free case)

$$\begin{aligned} \mathbf{y} &= \begin{bmatrix} \mathbf{a}_N(\lambda_1) \ldots \mathbf{a}_N(\lambda_K) \end{bmatrix}\begin{bmatrix} a_1 e^{j\phi_1} \\ \vdots \\ a_K e^{j\phi_K} \end{bmatrix} \\ &= \begin{bmatrix} \left\{ \frac{1}{2}\mathbf{a}_N(\lambda_1) + \mathbf{a}_N(\lambda_2) + \frac{1}{2}\mathbf{a}_N(\lambda_3) + \mathbf{a}_N(\lambda_4) + \cdots \right. \\ \left. + \mathbf{a}_N(\lambda_7) \right\}, \mathbf{a}_N(\lambda_8), \ldots, \mathbf{a}_N(\lambda_K) \end{bmatrix}\begin{bmatrix} a e^{j\phi} \\ a_8 e^{j\phi_8} \\ \vdots \\ a_K e^{j\phi_K} \end{bmatrix} \triangleq \mathbf{A}\mathbf{\Theta}. \end{aligned} \tag{A.37}$$

From the least-squares estimate of $\mathbf{\Theta}$ above

$$\mathbf{\Theta} = (\mathbf{A}^*\mathbf{A})^{-1}\mathbf{A}^*\mathbf{y}, \tag{A.38}$$

we directly obtain the estimates for the amplitudes $\{a_k\}_{k=1}^K$ and phases $\{\phi_k\}_{k=1}^K$.

References

[1] Z. Bi, P. Bruner, J. Li, K.N. Scott, Z. Liu, C.B. Stopka, H. Kim, D.C. Wilson, Spectral fitting of NMR spectra using an alternating optimization method with a priori knowledge, J. Magn. Reson. 140 (1999) 108–119.

[2] J.W.C. van der Veen, R. de Beer, P.R. Luyten, D. van Ormondt, Accurate quantification of in vivo 31-P NMR signals using the variable projection method and prior knowledge, Magn. Reson. Med. 6 (1988) 92–98.

[3] S. Cavassila, S. Deval, C. Huegen, D. van Ormondt, D. Graveron-Demilly, The beneficial influence of prior knowledge on the quantitation of in vivo magnetic resonance spectroscopy signals, Invest. Radiol. 34 (3) (1999) 242–246.

[4] S. Cavassila, S. Deval, C. Huegen, D. van Ormondt, D. Graveron-Demilly, Cramer–Rao bounds: an evaluation tool for quantitation, NMR Biomed. 14 (2001) 278–283.

[5] H. Barkhuysen, R. de Beer, W.M.M.J. Bovee, D. van Ormondt, Retrieval of frequencies, amplitudes, damping factors, and phases from time-domain signals using a linear least-squares procedure, J. Magn. Reson. 61 (1985) 465–481.
[6] H. Barkhuysen, R. de Beer, D. van Ormondt, Improved algorithm for noniterative time-domain model fitting to exponentially damped magnetic resonance signals, J. Magn. Reson. 73 (1987) 553–557.
[7] G.H. Golub, C.F. Van Loan, Matrix Computations, third ed., The Johns Hopkins University Press, Baltimore, MD, 1996.
[8] S. Van Huffel, J. Vandewalle, The Total Least-Squares Problem: Computational Aspects and Analysis, in: Frontiers in Applied Mathematics Series, vol. 9, SIAM, Philadelphia, 1991.
[9] S. Van Huffel, H. Chen, C. Decanniere, P. Van Hecke, Algorithm for time-domain NMR data fitting based on total least squares, J. Magn. Reson. A 110 (1994) 228–237.
[10] H. Chen, S. Van Huffel, D. van Ormondt, R. de Beer, Parameter estimation with prior knowledge of known signal poles for the quantification of NMR data in the time domain, J. Magn. Reson. A 119 (1996) 225–234.
[11] H. Chen, S. Van Huffel, Ad van den Boom, Paul van den Bosch, Subspace-based parameter estimation of exponentially damped sinusoids using prior knowledge of frequency and phase, Signal Process. 59 (1997) 129–136.
[12] S. Van Huffel, D. van Ormondt, Subspace-based exponential data modelling using prior knowledge, in: Proceedings Signal Processing Symposium, IEEE Benelux Signal Processing Chapter (SPS 98), Leuven, Belgium, March 26–27, 1998, pp. 211–214.
[13] S. Van Huffel, L. Lagae, L. Vanhamme, P. Van Hecke, D. van Ormondt, Improving blackbox MRS data quantification by means of prior knowledge, Abstracts of the 15th Annual Meeting European Society for Magnetic Resonance in Medicine and Biology (ESMRMB 98), Geneva, Switzerland, September 17–20, 1998, paper no. 44, published in Magnetic Resonance Materials in Physics, Biology and Medicine (MAGMA), vol. 6, Suppl. 1, September 1998, p. 13.
[14] Y. Selén, P. Stoica, N. Sandgren, S. Van Huffel, Using prior knowledge in SVD-based NMR spectroscopy—the ATP Example, in: Proceedings of the 7th International Symposium on Signal Processing and its Applications (ISSPA '03), Paris, France, July 1–4, 2003.
[15] L. Vanhamme, A. van den Boogaart, S. Van Huffel, Improved method for accurate and efficient quantification of MRS data with use of prior knowledge, J. Magn. Reson. 129 (1997) 35–43.
[16] P. Stoica, R. Moses, Introduction to Spectral Analysis, Prentice-Hall, Upper Saddle River, NJ, USA, 1997.
[17] T. Laudadio, N. Mastronardi, L. Vanhamme, P. Van Hecke, S. Van Huffel, Improved Lanczos algorithms for blackbox MRS data quantitation, J. Magn. Reson. 157 (2002) 292–297.
[18] G. Schwartz, Estimating the dimension of a model, Ann. Stat. 6 (1978) 461–464.
[19] J. Rissanen, Modelling by shortest data description, Automatica 14 (1978) 465–471.